Current Trends in Biotechnology and Pharmacy
Vol. 13 (2) 124-145, April 2019, ISSN 0973-8916 (Print), 2230-7303 (Online)

Quantitative Structure-activity Relationship based Design, Synthesis, and Evaluation of Novel Diarylether Derivatives as a potent Acetylcholinesterase inhibitor and Antioxidant to treat Cognitive dysfunctions

Pavan Srivastava[a], Prabhash Nath Tripathi[a], Piyoosh Sharma[a] and Sushant K Shrivastava[a]*

[a]Pharmaceutical Chemistry Research Laboratory, Department of Pharmaceutical Engineering and Technology, Indian Institute of Technology (Banaras Hindu University), Varanasi-221005, U.P., India.
*For Correspondence - skshrivastava.phe@itbhu.ac.in

Abstract

Some promising acetylcholinesterase (AChE) inhibitors with an antioxidant potential were designed, synthesised, and evaluated for their role in treating cognitive dysfunctions. The *in silico* Gaussian-based quantitative structure-activity relationship (QSAR), virtual screening (VS), QikProp drug-likeliness prediction and docking pose filtration protocols were adapted to design and screen the novel series of diaryl ether derivatives. Further, the selected compounds were investigated for their molecular binding stability using molecular dynamics (MD) simulation analysis and molecular mechanics generalised born surface area (MM-GBSA). The identified hits were synthesised and evaluated for their *in vitro* AChE inhibition and antioxidant potential. Among all the synthesized compounds, the compound 39 was observed as potent AChE inhibitor (AChE IC_{50} = 1.30 ± 0.09 µm; Ki = 0.054 ± 0.009 µM), and also the antioxidant potential of compound 39 (52.9%) was observed significantly better than standard donepezil (<10%) and parallel to ascorbic acid (56.6%). Further, compound 39 ameliorated the scopolamine-induced cognitive impairment in the Y-maze and passive avoidance testsin mice models. *Ex vivo* and biochemical analysis established the brain AChE inhibitory potential and antioxidant properties of compound 39. The results signified compound 39 to be a promising lead for the treatment of cognitive dysfunctions.

Key words: QSAR; virtual screening; diaryl ether; acetylcholinesterase; antioxidant.

1. Introduction

The incidences of dementia due to Alzheimer's disease (AD) and other neurodegenerative disorders are increasing alarmingly with a rate of nearly ten million new cases per year(1). According to the World Health Organisation's report, approximately fifty million people around the globe are currently suffering from dementia(2), and these numbers are expected to increase drastically in the future. The lack of effective therapies for these neurodegenerative disorders creates an enormous burden on society.

The initial cognitive impairment (starting stage of dementia) is a transitional state between the decline in cognition (with ageing) and the early stage of neurodegenerative disease (3). The early interventional therapies at the primary stage may reduce the progression of AD and other neurodegenerative diseases.

The parasympathetic neurotransmitter acetylcholine (ACh) has been shown to strengthen the synaptogenesis of active neurons and the up-regulation of cognitive functions(4, 5). ACh is hydrolysed by acetylcholinesterase (AChE) into choline and acetic acid. The inhibitors of AChE impede the breakdown of ACh and improve the amount of neuronal ACh (6). Currently, AChE

inhibitors AChEIs are the first line therapeutics to be used to treat the AD worldwide. The other cholinesterase is butyrylcholinesterase (BChE), which is found in both the plasma and brain and is also capable of hydrolysing ACh and the other esters (7).

The studies revealed that an imbalance of reactive oxygen species (ROS) causes oxidative stress and could also promote dementia(8). Antioxidants enhance cognition by suppressing ROS during the early stages of dementia(9). However, all the trials based on using a single target to develop a new drug to treat dementia have failed in the last two decades (10).Therefore, investigating multi-targeted ligands that can act on two or more targets is an alternative strategy to treat dementia. Considering the significance of AChE and the oxidative stress hypothesis, the investigation of AChEIs with an antioxidant potential could be a promising strategy for the treatment of dementia.

In the pursuit towards the search for novel multi-targeted ligands, several studies have revealed that the diaryl ether presented in various natural and synthetic pharmaceuticals could be a good sub-structure for the design of novel compounds. Apart from its wide range of pharmacological activities, various derivatives were extensively studied for AChEIs (11-14) and antioxidants (15).

Herein, we designed new molecules using the contour maps generated from the field-based quantitative structure-activity relationship (QSAR). Moreover, selected compounds using *in silico* screening protocols like docking, drug likeliness, molecular mechanics generalised born surface area (MM-GBSA) and molecular dynamics (MD) studies were identified and synthesised. The screened potential hits were evaluated for their *in vitro* cholinesterase inhibition, propidium iodide (PI) displacement assay and antioxidant potential followed by *in vivo* Y-maze and passive avoidance tests, *ex vivo* AChE estimation and antioxidant potential.

2. Results and Discussion

Computational Studies

Gaussian-based QSAR investigation and designing considerations

The field-based QSAR method was performed with a definite set of parameters to calculate the Gaussian equations using electrostatic fields, steric fields, hydrophobic fields, hydrogen bond donor (HBD) and acceptor (HBA) fields. The partial least-squares (PLS) fitting procedure was used to establish the relationship between these five fields. A set comprising of thirty-four known AChEIs (12, 16) with IC_{50} data ranging from a low to high micromolar concentration was selected for training and test sets. Further, their pIC_{50} was calculated usingthe reported procedure to generate the QSAR model (17) (Table 1). The model resulted in the field fraction values 0.09, 0.38, 0.27, 0.14, and 0.10 that showed the contributions of the electrostatic, steric, hydrophobic, HBD, and HBA respectively. It was noteworthy that, steric and hydrophobic fields gave much higher field fractions indicating the steric and non-polar features as major contributors. The results of the PLS method have a high value for a leave-one-out cross-validation q^2 (q^2> 0.2) and a non-cross-validation r^2 (0.54 and 0.98), respectively. The other PLS statistics and field Gaussian parameter were also found within the range, which proposed that the QSAR model has a good predictive ability and were statistically significant. The correlation of the observed pIC_{50} values and estimated pIC_{50} values of the best model was plotted, and a significant correlation was observed.

The designing consideration was focused on the electrostatic, steric, hydrophobic, HBD, and HBAinformation as observed through the contour maps from the generated model based on diaryl ether nucleus. The contour map around the molecule with the highest activity was generated by plotting the various coefficients from the model.

The study of contour map around the most active compound **5** (AChE IC_{50} = 2.5 µM) gave a

Vol. 13 (2) 124-145, April 2019, ISSN 0973-8916 (Print), 2230-7303 (Online)

fair idea about the modification required to increase the activity of parent compound (Fig. 1). This information was much valuable and suggested about the modification required to improve the activityof compound **5** (Fig. 2). Thus, four series were designed on the basis of information obtained through contour maps. In the I series, 1-chloro-3-nitro-2-phenoxybenzene, 3-chloro- 2-phenoxyaniline, 3-chloro-N-methyl-2-phenoxyaniline, and 3-chloro-N,N-dimethyl-2-phenoxyaniline were linked with the aromatic ring. In the III series, Schiff bases derivatives of amino acid methyl ester were designed. While, in the II and IV series, the reduced imines of the above compounds were designed. For ortho, meta, and para aromatic substitutions, we used various substituents from a different quadrant of the Craig plot. The substituents of the Craig plot were divided into four quadrants as per their hydrophobicity constant (π) on the X-axis and Hammett constant (σ)electron donor or acceptor on the Y-axis properties(18). Thus, a total of 698 molecules including the un-substituted derivatives were designed for the next VS, QikProp drug-likeliness prediction and docking studies(Fig*. 3).*

In silico molecular docking study : The virtual screening of these derivatives was carried out in the glide module of Schrodinger to predict their consensual interaction at the active site of cholinesterase enzyme. To screen the best compound, the new 698 designed compounds were docked at the active site of AChE (PDB: 1EVE).

The crystal structure of enzyme revealed that the detailed understanding of active binding sites has a critical role in the designing of novel inhibitors for the treatment of AD. Amongst the various residues, the amino acids involved in the catalytic active site (CAS) and peripheral anionic site (PAS) were the most important and selected as a primary criterion of docking post processing for screening the potential hits. The docking result showed compounds of series I, II, and III having nitro group had significant interaction at PAS region of the AChE binding pocket in comparison

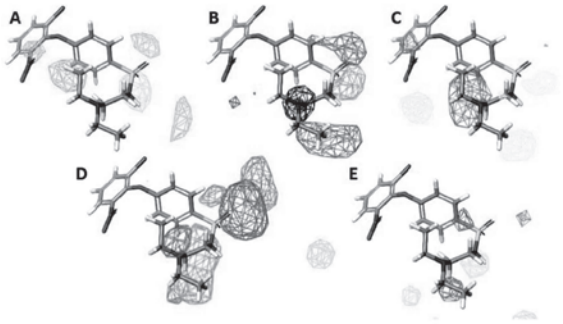

Fig. 1. Contour maps for the Gaussian-based QSAR model forcompound5 (A) Steric contour map, green (positive). (B) Electrostaticsteric contour map, blue (positive) and red (negative)(C) Hydrophobicsteric contour map, yellow (positive) and maroon(negative). (D) HBA contour map, orange (positive) and magenta(negative). (E)HBD contour region, sky blue(positive) and violet(negative).

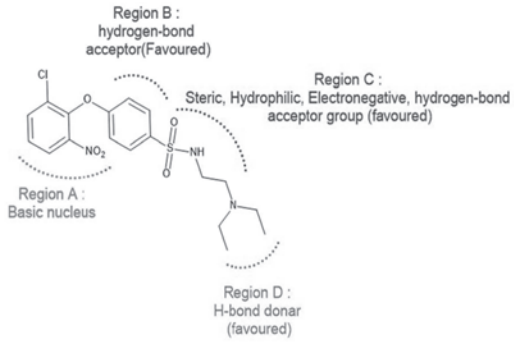

Fig. 2. Summary of favored information obtained from contour map around the most active compound 5.

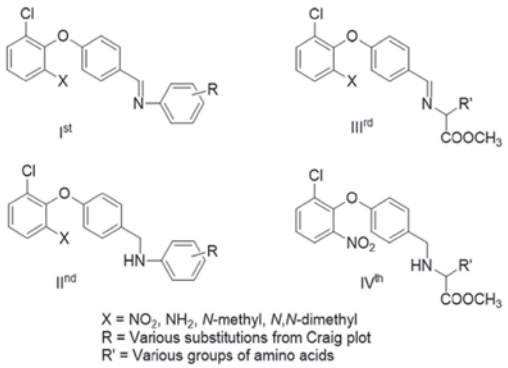

Fig. 3. Structures of designed compounds.

to the other designed compounds. The nitro and bromo group from the first quadrant (σ, π), COOH group from the second quadrant (σ, -π), hydroxylgroup from the third quadrant (-σ, -π), and isopropyl group from the fourth quadrant (-σ, π) were shown best interaction among the different substituents. It was also noted that the para-substituted compounds were shown better interaction in comparison the meta or ortho substitution. Similarly, in the designed Schiff bases derivatives of serine, threonine, and tyrosine methyl esters had shown the best interaction. Thus, 15 compounds out of 698 designed compounds were selected for the next step on the basis of their significant interaction at the active site of the AChE.The binding model of compound **39**, compound **5,** and donepezil against AChE were represented in figure 4A, 4B, and 4C respectively

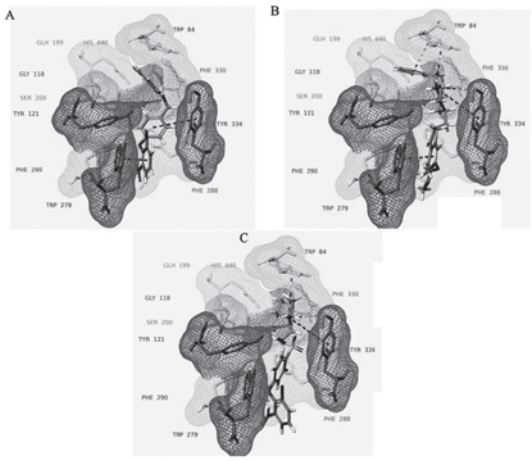

Fig. 4. *In silico* molecular docking simulations analysis of (A) The complex structure of compound 39 with AChE; (B) The complex structure of donepezil with AChE; (C) The complex structure of compound 5 with AChE; Red color represents the catalytic triad. Green color represents the anionic subsite site. Sky blue color represents acyl binding site. Purple color represents the PAS site. Graycolor represents the oxyanion hole. Receptor grid surface was generated around 5 Å distance. p-p interactions were represented by the red color dotted stick. p-cation interactions were represented by the green color dotted stick.

***In silico* drug-likeliness :** The drug likeliness physicochemical parameters i.e., caco-2 cell permeability (PPCaco), brain/blood partition coefficient (log BB), and ADME/Tox were predicted through QikProp module of Schrodinger 2016-1. The result showed that all the designed compounds were satisfied the *in silico* likeliness parameters.

MM-GBSA assay : MM-GBSA was used to rationalize the virtual screening results and prioritize the docking poses(19). The binding energy of the all identified hits on AChE was evaluated using Prime MM-GBSA module of Schrodinger 2016-1. The results of MM- GBSA indicated significant binding of diaryl ether derivatives in AChE and in the range of -85.45 to -28.22 kcal/mol.

Molecular dynamics simulations : Molecular dynamic (MD) simulation study was carried out to monitor the structural variations in the form of ligand-protein interactions and conformations(20). Molecular dynamics simulation runs of 50 ns were performed for docked protein-ligand complexes of the compound 33, compound 39, and compound 45, as a representative compound from each series to confirm the stability and validate molecular docking. The ligand-protein RMSD observed in the course of simulation exhibited deviation for the early 10 ns, and 23 ns respectively for compound 39 and compound 45 due to the early protein structural stabilization. While the RMSD for compound 33 exhibited unstable dynamics during the whole simulation. The Simulation interaction diagram of all docked complex demonstrated the simulations and the interactions with respect to protein and ligand upto 50 ns. The backbone structural deviations values, observed for the latter phase were non-significant and observed under the range of (1.5-11 Å), (3-5 Å: Fig.5), and (2.5-4.3 Å) respectively for compound 33, 39, and 45 respectively.

Thus, the complexes in AChE for compound **39** and compound **45** exhibited a stable-state dynamics for the remaining period, indicated that the ligands were not left their initial binding site.

The results indicated that 50 ns of the simulation were enough for stabilizing these complexes. However, the dynamics study for compound **33** exhibited unstable RMSD with respect to the protein and its binding pocket and these results were further supported by their *in vitro* studies later.

The Protein-Ligand Contacts stacked bar chart for compound **39** in Fig.6&7 showed the normalized interactions including hydrophobic (Trp84, Trp279, Phe330, Phe331, Tyr334), H-bonding (Tyr121), water bridge (His440) and ionic interaction (Asp285). The Ligand-Protein Contacts diagram (Fig. 7) showed a schematic diagram of the compound **39** interacting with AChE during MD simulation. The stacked bar chart showed that compound **39** interacted with His440 (29%) at CAS and with Trp84 (65%), Phe330 (56%) at anionic subsite. The MD simulation of Serine Schiff base containing compound **45** showed 40% and 31% contact time with His440 and Ser200 respectively at CAS, with Trp121 (32%), and Tyr334 (35%) at PAS and with Phe330 (33%) at anionic subsite. The overall results of MD simulation indicated that amino acid residue of PAS and anionic subsite was contributing more toward the stabilization of diaryl nucleus and the results were in the accordance of docking studies.

Thus, based on the QSAR model, docking, drug likeliness, MM-GBSA, and dynamics studies, 15 compounds were screened and selected. Further using the best QSAR model, the activity of the designed compounds against AChE was generated (pIC_{50}). Predicted IC_{50} of newly designed compounds indicated that it would be effective to synthesize these molecules and further validate the model by testing them *in vitro*.

Chemistry : Diaryl ether derivative compound **23** was synthesized by reacting 1-chloro-2-fluoro-3-nitrobenzene with parahydroxybenzaldehyde using Williamson ether synthesis(21). The sodium hydride was used as a strong base to generate the alkoxide ion from parahydroxybenzaldehyde in cold conditions. The formation of diaryl ether was well characterized by ^{1}H NMR and ^{13}C NMR spectroscopy. In the second step, the compound **23** was allowed to react with various amines (**24-29**) and amino acid esters (**45-47**) to form the Schiff base under acidic and basic conditions respectively. The compound (**30-35**) was further reduced to a secondary amine using sodium borohydride (**36-41**). The presence of Schiff base was confirmed by the characteristic singlet peak at 8-9 ppm, that and it was disappeared in the reduced compound with the appearance of two new peaks of CH_2 and NH proton at 4.4 ppm and 5.4 ppm respectively.

***In vitro* studies**

***In vitro* AChE Studies and structuralactivity relationship :** The Ellman's method (22) is a quick reliable and accurate procedure to check the rate of hydrolysis inhibited by the test compound using acetylthiocholine iodide as a substrate and DTNB as a reagent. All synthesized compounds were tested for the AChE inhibition. Compound 39 was found to be the most active (AChE IC_{50} = 1.30 ± 0.09 µM; BChE IC_{50} = 24.1 ± 0.9 µM). Almost all the designed fifteen compounds showed AChE inhibition property(except 32, 45, 46, and47) (AChE IC_{50} Range = 1.3 to >50 µM; BChE IC_{50} Range = 4.71 to >50 µM)(Table 2).

Propidium iodide (PI) is a PAS-AChE (fluorescent) specific inhibitor. When PI bounds to the PAS region of AChE resulted in the increased fluorescent intensity. If an inhibitor bound specifically to the PAS and displace the PI from PAS-AChE complex, resulted in decreased fluorescent intensity. Therefore, the best compound **39** was also studied for enzyme kinetic study and propidium iodide displacement assay (23). It displaces 14.4 % of propidium iodide from the PAS region confirms it's binding at PAS.The most active AChEI compound **39** was subjected to enzyme kinetic study which displayed competitive inhibition (Ki = 0.054 ± 0.009 µM) using Lineweaver–Burk plot (24).

The SAR of synthesized derivatives was summarized in figure 8. The *in vitro* studies showed that the modification in the basic 1-chloro-3-nitro-

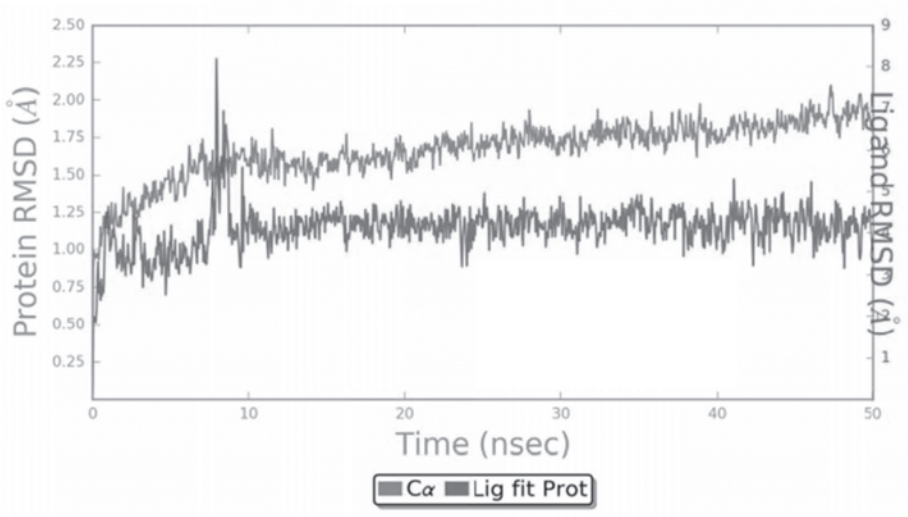

Fig 5. RMSD fluctuations of protein backbone (blue) and compound **39** (red) for 50 ns simulation run on AChE proteins.

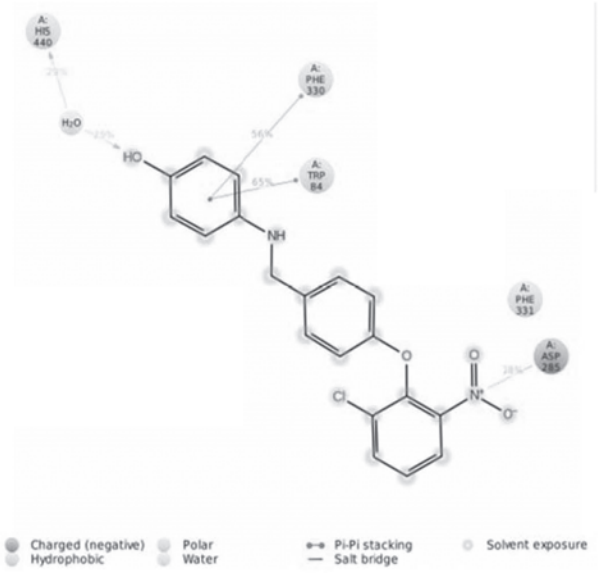

Fig. 6. A schematic representation showing the interaction of compound **39** with active siteamino acid residues of AChE.

Vol. 13 (2) 124-145, April 2019, ISSN 0973-8916 (Print), 2230-7303 (Online)

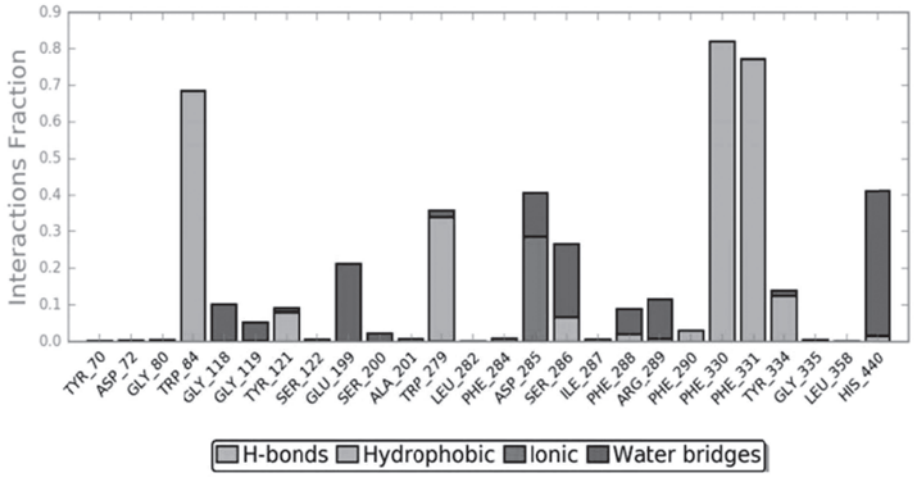

Fig. 7. Stacked bar chart representation of compound **39** with active site amino acidresidues of AChE showing different colors for different types of interactions (Green- H-bonding; Gray-Hydrophobic; Blue- Water bridges; Pink- Ionic interactions).

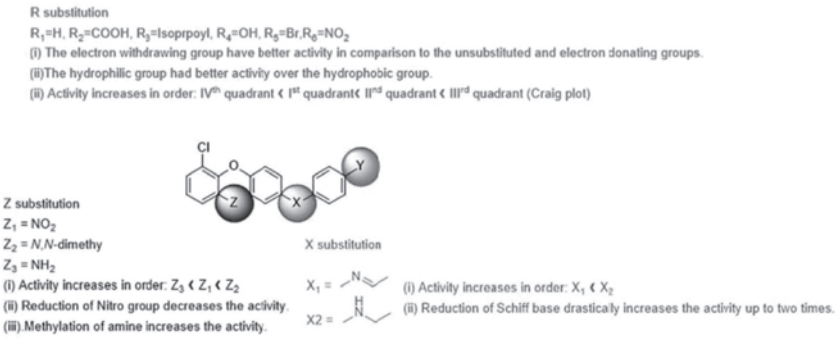

Figure 8. Structure-activity relationship (AChE)of diaryl ether derivatives.

2-phenoxybenzene reduces the activity. The structural-activity relationship (SAR) of compounds (**30-41**) indicated that the reduction of the Schiff base increases the activity two-fold. It was also observed that the para substitution increases the activity many folds as compared to unsubstituted analogs. Various substituents at the para position from the different quadrant of the Craig Plot provide significant insight intoSAR regarding the substitution required for AChE inhibition. The descending order activity is summarized as OH > COOH> NO_2>Br > isopropyl substitutions. Further, it was observed that the substitution from Ist Quadrant substitution (the electron withdrawing (ó) and hydrophobic substituent (ð)) was most active against AChE in comparison to the other quadrant substitution and the unsubstituted analogs. Further, the Schiff base of amino acid esters (**42-44)** (AChE IC_{50} = >50 µM; BChE IC_{50} = >50 µM) had not shown any significant inhibitory activity against AChE *in vitro*.

***In vitro* antioxidant studies and structural-activity relationship :** All the synthesized compounds were tested for its antioxidant activity using a quick and reliable 1,1-diphenyl-2-picrylhydrazyl (DPPH) method (25). The ascorbic

acid was used as the standard and around 10 compounds among 15 compounds exhibited significant antioxidant potential whereas the standard donepezil was not exhibited antioxidant activity (<10%). Interestingly, the compound **39** having highest AChE inhibition(AChE IC_{50} = 1.30 ± 0.09 µM) was also the compound with maximum antioxidant activity (52.9 ± 2.6 %) as compared to the ascorbic acid (56.6 ± 3.1 %).

The SAR indicated that the substituent, as well as spacer, affects the antioxidant activity. The imine had the lower antioxidant potential as compared to the methanamine spacer linked derivatives, and Schiff base derivative of amino acid esters. The various substitutions at the para position of the aromatic ringhave also influenced the activity. The phenolic OH group had the maximum antioxidant potential as compared to the other substitutions.

Blood-brain barrier permeation assay : The *in vitro* parallel artificial membrane permeability assay(26) (PAMPA) was performed for compound 39to predict its blood-brain barrier permeation. Verapamil, diazepam, progesterone, atenolol, dopamine, lomefloxacin, alprazolam, chlorpromazine, and oxazepam were used as controls (to validate the PAMPA-BBB model) to determine *in vitro* permeability (P_e) along with compound 39. P_e (10^{-6} cm s^{-1}) values greater than 4 signified the high permeability of compound. The donepezil (7.54 ± 0.42) and compounds 39 showed appreciable CNS permeability (5.57 ± 0.68).

***In vivo* studies**

Y-maze test : Y-maze spontaneous alternation experiment was used as the behavioral model to test the animal's spatial working memory. The animal was injected scopolamine to inhibit the memory before the commencement of the experiment and since the hippocampus was involved in the task of the model, Y-maze experiment directly indicated the improvement of learning and memory behavior of the mice treated with compound 39.

Spontaneous alteration score was determined for the compound **39** at three doses (1, 5, and 20 mg/kg) and compared to scopolamine, donepezil, and control-treated group (Fig. 9 A). The results showed improvement in alternation score at a dose of 5 mg/kg for compound **39.** Moreover, at the dose 1 mg/kg, donepezil showed significant alternations as compared to thescopolamine treated group.

The novel arm entry was performed to check the anxiety and cainophobia behaviors of mice (Fig. 9B). The mice treated with compound **39** had spent their most of period in exploring the new arm at the dose of 1 and 5 mg/kg, while the scopolamine-treated mice spend more time at the center of the maze. At the dose of 5 mg/kg, compound **39** showed significant differences with scopolamine treated group while the differences were not significant as compared to the donepezil. Thus, compounds **39** showed a significant increase in the working memory and declined in the anxiety without altering the locomotive behavior of mice.

Passive avoidance test : In passive avoidance test the shock was given in the acquisition phase and during the retention phase, transfer latency periods were recorded. The significant difference was observed in the transfer latency time for acquisition trail in comparison to the retention trial for the compound 39 (1, 5, and 20 mg/kg) and donepezil-treated group, while no significant difference was observed for the scopolamine treated group (Figure 9C). Thus compound 39 exhibited a significant increase in transfer latency time in comparison to scopolamine treated group.

Rotarod performance test : The rotarod study was performed to examine the motor learning and motor coordination of the animals. Treatment groups were tested for fall off time (seconds) before and after treatment by rotarod apparatus to check the neurotoxicity. The compound 39 showed the non-significant difference between fall off time before and after treatment on rota rods suggestive of the lack of any side effect on the motor system

of the animals, while diazepam treated group was observed to be neurotoxic.

Neurochemical analysis

Ex vivo evaluation of AChE : The rate of hydrolysis of ACh in the brain was determined for compound 39 (5 mg/kg), donepezil, control, and scopolamine treated group in the *ex vivo* experiment using the Ellman assay protocol. The results revealed that there was a significant difference in the rate of hydrolysis for compound39 (5 mg/kg) and donepezil compared to the scopolamine treated group (Figure 10A). These results also reflected the ability of compound 39 to cross the blood-brain barrier.

***Ex vivo* evaluation of oxidative stress biomarkers :** To evaluate the antioxidant potential, we had performed different *ex vivo*

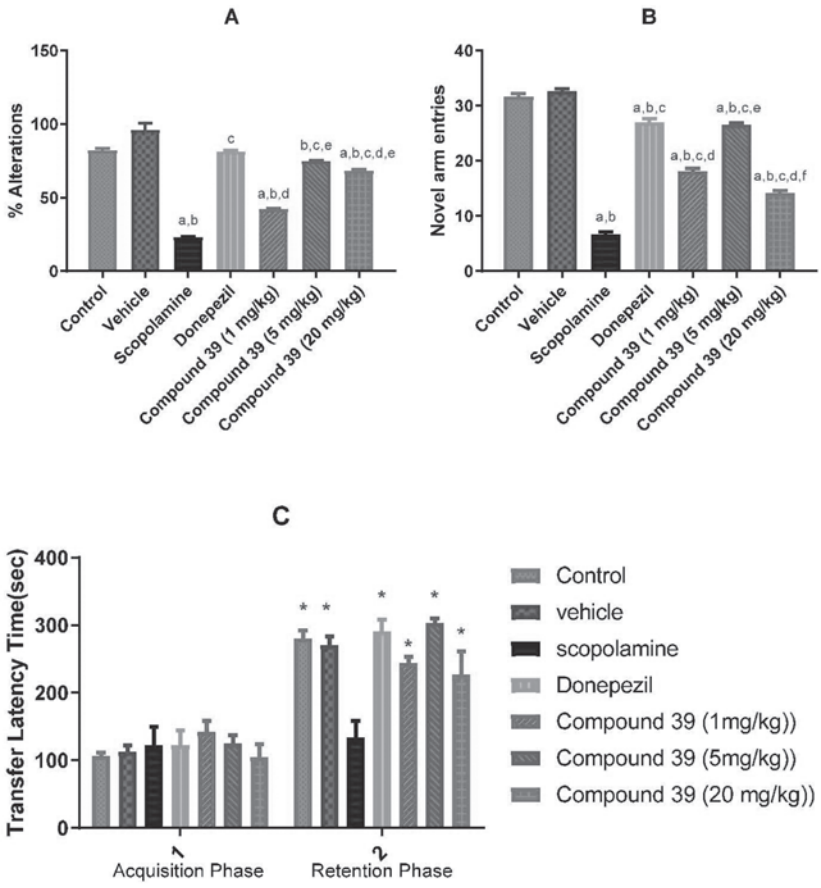

Fig. 9. The in vivo learning and memory test effect of compound 39+ scopolamine (1, 5 , and 20 mg/kg), donepezil (1 mg/kg) and scopolamine (A) Percentage alteration; (B) novel arm entry; Values were expressed as Mean ± SEM, n=6, a $p<0.05$ compared to control; b $p<0.05$ compared to vehicle; c $p<0.05$ compared to scopolamine; d $p<0.05$ compared to donepezil + scopolamine; e $p<0.05$ compared to compound 39+ scopolamine at dose of 1 mg/kg; f $p<0.05$ compared to compound 39+ scopolamine at dose of 5 mg/kg.Values were expressed as ± SEM; Significance wasdetermined by one-way ANOVA, followed by Tukey's test. (C) The effect of scopolamine-induced alteration in the passive avoidance Test. Values are expressed as ± SEM (n = 6); Significance was determined by two-way ANOVA, followed by Tukey's test.* $p<0.001$ compared to respective acquisition Trial.

Vol. 13 (2) 124-145, April 2019, ISSN 0973-8916 (Print), 2230-7303 (Online)

biochemical test including thiobarbituric acid (TBA) assay, hydrogen peroxide (H_2O_2) assay, reduced glutathione (GSH) assay, superoxide dismutase (SOD) assay to determine malonaldehyde (MDA)/mg protein, catalase activity, GSH level, nitrite level, and SOD unit/mg protein respectively for control, scopolamine, compound 39 (5 mg/kg dose), and donepezil-treated group to check their effect on oxidative stress.

The *ex vivo* experiment showed a significant decreased oxidative stress among the group treated with compound **39**(5 mg/kg) as compared to donepezil and scopolamine treated group, revealing its antioxidant property (Fig. 10B-10F). However, the donepezil-treated group showed no improvement in oxidative stress and found non-significant as compared to scopolamine treated group. Hence, the compound **39** was found to be better than donepezil concerning counteracting oxidative stress induced by scopolamine along with improved learning and memory.

3. Conclusion

Some diaryl ether derivatives were computationally designed and synthesized as potential AChE inhibitor with significant antioxidant property parallel to ascorbic acid. We have evaluated the most potent compound for improving the learning and memory behavior and the results were compared with the standard drug donepezil. Since the design of the molecules was based on Craig plot and Gaussian-based QSAR, therefore, their structure-activity relationship gave useful insights to further enhance and modify the potential of molecules in the future. The most potent compound **39** showed the significant reversal of cognitive deficits and antioxidant potential at the dose of 5 mg/kg, compared to standard drug donepezil in animal models. These results also showed the excellent predictive ability

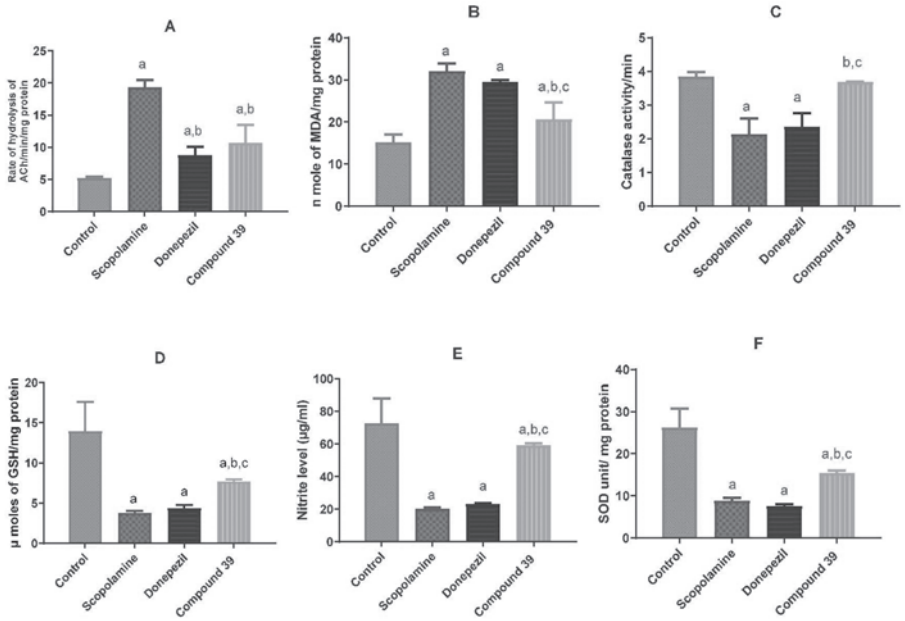

Fig. 10. The ex vivoAChE and antioxidant effect of compound 39 (5 mg/kg), donepezil (1 mg/kg) and scopolamine(A)Rate of hydrolysis of ACh; (B) Lipid peroxidation assay; (C) Catalase activity; (D) Reduced glutathione assay; (E) Nitrite level (F) Superoxide dismutase (SOD) assay; a $p<0.05$ compared to control; b $p<0.05$ compared to scopolamine; c $p<0.05$ compared to donepezil. Values are expressed as Mean ± SEM; Significance was determined by one-way ANOVA, followed by Tukey's test.

Vol. 13 (2) 124-145, April 2019, ISSN 0973-8916 (Print), 2230-7303 (Online)

Table 1. Compound structure,pIC_{50}, and results of Gaussian QSAR model.

Compound Number	Structure	Set	pIC_{50}
1[a]	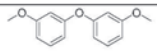	training	7.72
2[a]	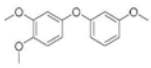	test	7.92
3[a]	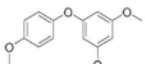	training	7.77
4[a]	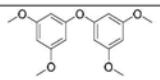	test	7.81
5[b]	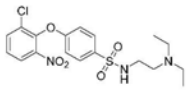	training	5.60
6[c]	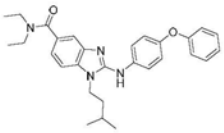	training	4.41
7[c]	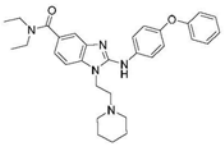	training	2.90
8[d]	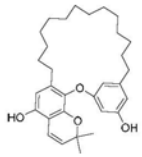	training	5.46
9[d]	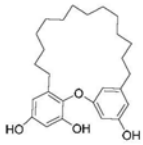	test	5.46
10[d]	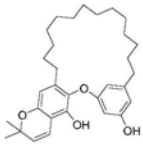	training	5.44

11[e]	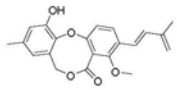	test	5.79
12[e]	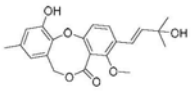	training	3.00
13[e]	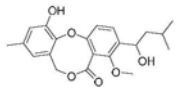	training	3.00
14[e]	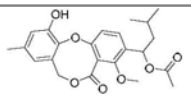	training	3.00
15[e]	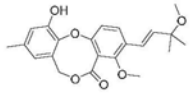	training	3.00
16[f]	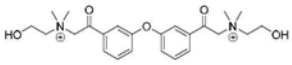	training	2.99
17[f]	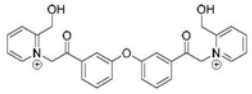	test	3.10
18[f]	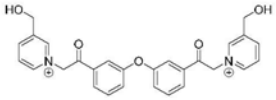	training	5.53
19[f]	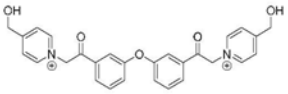	training	4.92
20[f]	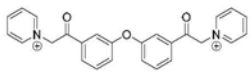	test	5.49

[a](11), [b](12), [c](13), [d](40), [e](41), [f](14)

and accuracy of our Gaussian-based 3D-QSAR model. Thus, the present study provided a useful class of AChE inhibitors having antioxidant potential with promising therapeutic applications against dementia.

4. Material and Methods

Computational study : Field-based 3D QSAR, Molecular docking, QikProp Molecular Mechanics-Generalized Born Surface Area (MM-GBSA) approach and molecular dynamics studies were performed on Phase, Glide, QikProp, Prime, and Desmond modules of Schrodinger 2018-1 respectively using the standard protocol and following the procedure adopted before (27, 28). The crystallographic structures of human AChE in complex with donepezil available in the protein data bank (PDB) (http://www.rcsb.org/pdb/home/home.do) were selected with accession codes 1EVE.

Chemistry

Instrumentation and chemicals : FT-IR spectra were recorded on Bruker ECO-ATR (Alpha). ^{1}H-NMR (500 MHz) and ^{13}C-NMR spectra (125 MHz) were recorded on a BrukerAvance FT-NMR spectrophotometer at room temperature using TMS as an internal standard. Elemental analyses (C, H, N) were performed using EXETER CE-440. All the chemicals were purchased from Sigma-Aldrich (India) and were used without further purification. Thin layer chromatography monitored the progress of the reactions on Merck silica gel 60 F254 aluminum sheets (Merck, Germany).

Synthesis : Synthesis of 4-(2-chloro-6-nitrophenoxy)benzaldehyde (23): 4-hydroxy-benzaldehyde (22) (0.040 mol) and 1-chloro-2-fluoro-3-nitrobenzene (21) (0.040 mol) was dissolved in THF in cold condition followed by portion wise addition of sodium hydride (60 % dispersion in mineral oil; 0.040 mol) in reaction. The reaction mixture was stirred at room temperature under inert atmosphere for 4 h. Completion of the reaction was monitored by TLC. After the completion of the reaction, the solvent was evaporated and the product was extracted using ethyl acetate. The organic layer was evaporated and subjected to column chromatography using 10% EtOAc/Hexane to afford the product 4-(2-chloro-6-nitrophenoxy) benzaldehyde (23). Yield 90%; ^{1}H NMR (500 MHz, DMSO-d_6) **δ** 9.92 (s, 1H), 8.19 (m, 1H), 8.17 (m, 1H), 8.09 – 7.92 (m, 2H), 7.66 (m, 1H), 7.11 – 7.09 (m, 2H).^{13}C NMR (125 MHz, DMSO-d_6) **δ** 191.99, 159.74, 144.88, 140.31, 134.31, 132.81, 132.58, 132.19, 128.38, 126.85, 126.04, 118.94, 118.73; Anal. $C_{13}H_8ClNO_4$: C, 56.24; H, 2.90; N, 5.04; Found: C, 56.27; H, 2.84; N, 5.01.

General preparation for the synthesis of compounds (30-35) (29) : The compound 23 (0.003 mol) was refluxed with various amines (0.003 mol, 24-29) using two drops of glacial acetic acid as catalyst and ethanol as a solvent. The reaction mixture was refluxed until the completion of the reaction. After completion of the reaction, the solvent was evaporated and recrystallized using methanol to obtain the target compounds (30-35).

1-(4-(2-chloro-6-nitrophenoxy)phenyl)-N-phenylmethanimine (30): ^{1}H NMR (500 MHz, $CDCl_3$) **δ** ^{1}H NMR (500 MHz, Chloroform) **δ** 8.54 (s, 1H), 7.95 (m, 1H), 7.64 (m, 1H), 7.58 – 7.44 (m, 2H), 7.35 – 7.28 (m, 4H), 7.24 (m, 2H), 7.08 – 6.93 (m, 2H). ^{13}C NMR (125 MHz, $CDCl_3$) **δ** 163.06, 158.22, 151.07, 144.88, 140.31, 133.07, 132.81, 131.21 – 130.81, 129.42,129.02, 128.38, 126.85, 126.04, 125.41, 121.29, 121.08, 120.23, 119.84 ; Anal. $C_{19}H_{13}ClN_2O_3$: C, 64.69; H, 3.71; N, 7.94; Found: C, 64.65; H, 3.76; N, 7.95.

4-((4-(2-chloro-6-nitrophenoxy) benzylidene) amino) benzoic acid (31): ^{1}H NMR (500 MHz, DMSO-d_6) **δ** 12.45 (s, 1H), 8.80 (s, 1H), 8.15 – 7.97 (m, 3H), 7.73 – 7.54 (m, 3H), 7.54 – 7.45 (m, 2H), 7.26 (m, 1H), 7.01 – 6.86 (m, 2H). ^{13}C NMR (125 MHz, DMSO-d_6) **δ** 168.95 , 163.06 , 158.22 , 158.04 , 144.88 , 140.31 , 133.07 , 132.81 , 131.68, 131.46 , 131.21, 130.81, 128.38, 127.93, 126.8, 126.04, 120.23, 119.84, 117.48, 117.26 ; Anal. $C_{20}H_{13}ClN_2O_5$: C, 60.54; H, 3.30; N, 7.06; Found : C, 60.51; H, 3.26; N, 7.10.

1-(4-(2-chloro-6-nitrophenoxy) phenyl)-N-(4-isopropylphenyl)methanimine (32): ^{1}H NMR (500

Table 2. IC_{50} values of the synthesized derivatives and antioxidant activity.

Comp. code	AChE IC_{50} (μM) ± SEM	BChE IC_{50} (μM) ± SEM	Selectivity Index[a]	Reduction % of DPPH ± SEM at 10 μM
30	40.7 ± 2.1 μM	>50 μM	-	<10%
31	5.6 ± 0.3 μM	34.9 ± 1.4 μM	6.20 ± 0.5	<10%
32	>50 μM	>50 μM	-	<10%
33	2.3 ± 0.12 μM	14.9 ± 0.7 μM	6.47 ± 0.4	41.5 ± 2.3
34	7.8 ± 0.8 μM	>50 μM	-	<10%
35	12.2 ± 1.1 μM	27.0 ± 2.0 μM	2.2 ± 0.8	<10%
36	20.3 ± 1.4 μM	>50 μM	-	25.5 ± 2.6
37	1.7 ± 0.09 μM	15.3 ± 1.1 μM	9.0 ± 0.9	26.8 ± 0.6
38	48.5 ± 3.3 μM	>50 μM	-	23.2 ± 1.1
39	1.3 ± 0.09 μM	24.1 ± 0.9 μM	18.5 ± 1.2	52.9 ± 2.6
40	16.5 ± 1.6 μM	>50 μM	-	28.1 ± 2.0
41	12.2 ± 1.0 μM	4.71 ± 0.13	0.38 ± 0.04	26.1 ± 1.2
45	>50 μM	>50 μM	-	18.7 ± 1.1
46	>50 μM	>50 μM	-	18.0 ± 0.6
47	>50 μM	>50 μM	-	45.5 ± 2.5
Donepezil*	0.04 ± 0.01	15.24 ± 0.88	381 ± 6.33	<10%
Ascorbic acid	nd	nd	nd	56.6 ± 3.1

Values are expressed in the mean ± SEM (n=3); [a]IC_{50}(BChE)/IC_{50}(AChE); nd (not determined)

MHz, $CDCl_3$) δ 8.53 (s, 1H), 7.94 (m, 1H), 7.64 (m, 1H), 7.58 – 7.43 (m, 2H), 7.36 – 7.23 (m, 5H), 7.09 – 6.94 (m, 2H), 3.07 (m, 1H), 1.41 – 1.27 (d, 6H). ^{13}C NMR (125 MHz, $CDCl_3$) δ 163.06, 158.22, 148.50, 145.86, 144.88, 140.31, 133.07, 132.81, 131.21, 130.81, 128.38, 126.85, 126.66, 126.45, 126.04, 123.56, 123.16, 120.23, 119.84, 34.20, 23.57, 23.17 Anal. $C_{22}H_{19}ClN_2O_3$: C, 66.92; H, 4.85; N, 7.09; Found: C, 66.89; H, 4.81; N, 7.13.

4-((4-(2-chloro-6-nitrophenoxy) benzylidene)amino) phenol (33)

^{1}H NMR (500 MHz, $CDCl_3$) ä 8.59 (s, 1H), 7.93 (m, 1H), 7.93 – 7.75 (m, 4H), 7.40 (m, 1H), 7.75 (m, 1H), 7.15 – 7.14 (m, 3H), 6.92 (m, 1H), 4.65 (s, 1H).^{13}C NMR (125 MHz, $CDCl_3$) δ 163.06 , 158.18 (d), 144.81 (d), 140.31 , 133.07 , 132.81 , 131.21, 130.81 , 128.38 , 126.85 , 126.04, 122.78, 122.57, 120.23, 119.84, 116.98, 116.77 ; Anal. $C_{19}H_{13}ClN_2O_4$: C, 61.88; H, 3.55; N, 7.60; Found: C, 61.91; H, 3.51; N, 7.57.

N-(4-bromophenyl)-1-(4-(2-chloro-6-nitrophenoxy)phenyl)methanimine (34): ^{1}H NMR (500 MHz, $CDCl_3$) δ 8.60 (s, 1H), 7.95 (m, 1H), 7.65 (m, 1H), 7.62 – 7.45 (m, 4H), 7.27 – 7.16 (m, 3H), 7.10 – 6.96 (m, 2H). ^{13}C NMR (125 MHz, $CDCl_3$) δ 163.06 , 158.22 , 154.08, 144.88, 140.31, 133.07, 132.81, 132.09, 131.88, 131.21, 130.81, 128.38, 126.85, 126.04, 122.15, 121.93, 120.23, 119.84, 117.74 ; Anal. $C_{19}H_{12}BrClN_2O_3$: C, 52.87; H, 2.80; N, 6.49; Found: C, 52.83; H, 2.77; N, 6.43.

1-(4-(2-chloro-6-nitrophenoxy)phenyl)-N-(4-nitrophenyl)methanimine (35): ^{1}H NMR (500 MHz, $CDCl_3$) δ 8.56 (s, 1H), 8.26 – 8.12 (m, 2H), 7.94 (m, 1H), 7.63 (m, 1H), 7.62 – 7.44 (m, 4H), 7.24 (m, 1H), 7.07 – 6.93 (m, 2H). ^{13}C NMR (125 MHz, $CDCl_3$) ä 163.06, 158.22, 158.01, 144.88, 144.19, 140.31, 133.07, 132.81, 131.21, 130.81, 128.38, 126.85, 126.04, 125.58, 125.18, 121.67, 121.28, 120.23,119.84 ; Anal. $C_{19}H_{12}ClN_3O_5$: C, 57.37; H, 3.04; N, 10.56; Found: C, 57.40; H, 3.00; N, 10.51.

General preparation for the synthesis of compounds (36-41)(30): The compound 23 (0.003 mol) was refluxed with various respective amines (0.003 mol, 24-29) and ethanol as a solvent. The reaction mixture was refluxed until the completion of the reaction. After completion of the reaction, sodium borohydride (0.004 mol) was added portion wise with continuous stirring at 0–5 ^{0}C for 30 min. The solvent was evaporated after the completion of the reaction mixture and workup using ethyl acetate. The organic layer was evaporated and recrystallized using methanol to obtain the target compounds (36-41).

N-(4-(2-chloro-6-nitrophenoxy)benzyl)aniline (36): ^{1}H NMR (500 MHz, $CDCl_3$) δ 7.89 (m, 1H), 7.60 (m, 1H), 7.32 – 7.20 (m, 3H), 7.16 – 7.10 (m, 2H), 7.02 – 6.88 (m, 2H), 6.65 (m, 1H), 6.62 – 6.49 (m, 2H), 4.47 (d, 2H), 4.11 (s, 1H). ^{13}C NMR (125 MHz, $CDCl_3$) δ 154.77, 147.84, 144.88, 140.31, 134.53, 132.81, 129.31, 128.92, 128.38, 127.43, 127.22, 126.85, 126.04, 119.91, 119.52, 118.27, 114.35, 114.14, 46.86 ; Anal. $C_{19}H_{15}ClN_2O_3$: C, 64.32; H, 4.26; N, 7.90; Found: C, 64.29; H, 4.22; N, 7.87.

4-((4-(2-chloro-6-nitrophenoxy) benzyl)amino)benzoic acid (37)

^{1}H NMR (500 MHz, DMSO-d_6) ä 12.51 (s, 1H), ä 7.95 (m, 1H), 7.93 – 7.84 (m, 2H), 7.65 (m, 1H), 7.27 – 7.18 (m, 3H), 7.08 – 6.94 (m, 2H), 6.85 – 6.71 (m, 2H), 4.48 (d, 2H), 4.02 (s, 1H).^{13}C NMR (125 MHz, DMSO-d_6) δ 168.95, 154.96 – 154.66, 144.88, 140.31, 134.53, 132.81, 132.21, 132.00, 128.38, 127.43, 127.22, 126.85, 126.04, 120.79, 119.91, 119.52, 111.77, 111.37, 46.86 ; Anal. $C_{20}H_{15}ClN_2O_5$: C, 60.24; H, 3.79; N, 7.02; Found: C, 60.20; H, 3.81; N, 7.05.

N-(4-(2-chloro-6-nitrophenoxy)benzyl)-4-isopropylaniline (38): *^{1}H NMR (500 MHz, $CDCl_3$) ä 7.95 (m, 1H), 7.65 (m, 1H), 7.28 – 7.17 (m, 3H), 7.17 – 7.08 (m, 2H), 7.08 – 6.94 (m, 2H), 6.63 – 6.49 (m, 2H), 4.47 (d, 2H), 3.68 (s, 1H), 3.02 (s, 1H), 1.40 – 1.27 (m, 6H). ^{13}C NMR (125 MHz, $CDCl_3$) δ 154.77, 144.88, 143.59, 140.31, 138.11, 134.53, 132.81, 128.38, 128.25, 127.96, 127.43, 127.22, 126.85, 126.04, 119.91, 119.52, 116.60, 116.20, 46.86, 34.20, 23.57, 23.17 ; Anal. $C_{22}H_{21}ClN_2O_3$: C, 66.58; H, 5.33; N, 7.06; Found: C, 66.55; H, 5.36; N, 7.02.*

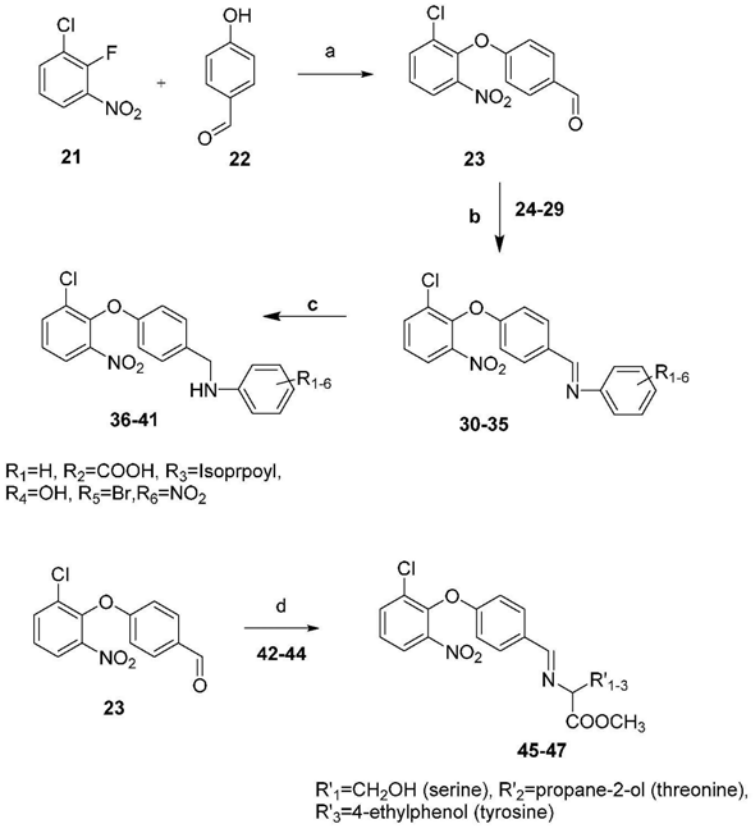

Scheme 1. Reagents and conditions: (a) THF, NaH, 25-35□C, 4 h; (b) ethanol, glacial acetic acid (catalytic amount) 60-65 □C, 12 h (**24-29** were various amines) . (c) ethanol, glacial acetic acid (catalytic amount), $NaBH_4$ 60-65 □C, 12 h; (d) ethanol, triethylamine, 60-65□C, 48 h 42-44 **47** were serine, threonine, and tyrosine methyl ester respectively).

4-((4-(2-chloro-6-nitrophenoxy) benzyl)amino) phenol (39):*^{1}H NMR (500 MHz, $CDCl_3$) δ 7.23 (m, 2H), 7.11 (m, 1H), 6.98 – 6.97 (m, 3H), 6.826 (m, 1H), 6.77 – 6.66 (m, 4H), 5.09 (s, 1H), 4.41 (d, 2H), 3.70 (s, 1H). ^{13}C NMR (125 MHz, $CDCl_3$) δ 154.77, 151.27, 144.88, 140.72, 140.31, 134.53, 132.81, 128.38, 127.43 – 127.22, 126.85, 126.04, 119.91, 119.52, 117.49, 117.27, 115.48, 115.27, 46.86 ; Anal. $C_{19}H_{15}ClN_2O_4$; C, 61.55; H, 4.08; N, 7.56; Found: C, 61.53; H, 4.06; N, 7.51.*

4-bromo-N-(4-(2-chloro-6-nitrophenoxy) benzyl)aniline (40)

^{1}H NMR (500 MHz, $CDCl_3$) δ 7.91 (m, 1H), 7.61 (m, 1H), 7.39 – 7.26 (m, 2H), 7.26 – 7.15 (m, 3H), 7.01 – 6.87 (m, 2H), 6.51 – 6.37 (m, 2H), 4.47 (d, 2H), 4.00 (s, 1H).^{13}C NMR (125 MHz, $CDCl_3$) δ 154.77, 146.78, 144.88, 140.31, 134.53, 132.81, 132.14 – 131.75, 128.38, 127.43, 127.22, 126.85, 126.04, 119.91, 119.52, 115.59, 115.19, 109.18, 46.86 ; Anal. $C_{19}H_{14}BrClN_2O_3$: C, 52.62;

H, 3.25; N, 6.46; Found: : C, 52.58; H, 3.21; N, 6.42.

4-bromo-N-(4-(2-chloro-6-nitrophenoxy) benzyl) aniline (41)

^{1}H NMR (500 MHz, $CDCl_3$) δ 8.15 – 8.03 (m, 2H), 7.95 (m, 1H), 7.65 (m, 1H), 7.27 – 7.18 (m, 3H), 7.08 – 6.94 (m, 2H), 6.93 – 6.79 (m, 2H), 4.48 (d, 2H), 3.89 (s, 1H).^{13}C NMR (125 MHz, $CDCl_3$) δ 156.36, 154.77, 144.88, 140.31, 138.13, 134.53, 132.81, 128.38, 127.43, 127.22 ,126.85, 126.04, 125.56, 125.34, 119.91, 119.52, 114.50, 114.11, 46.86 ; Anal. $C_{19}H_{14}BrClN_2O_3$: C, 57.08; H, 3.53; N, 10.51; Found: C, 57.05; H, 3.55; N, 10.53.

General preparation for the synthesis of compounds (45-47) (31)

Various amino acid esters (0.003 mol, 42-44) were dissolved in ethanol and reaction mixture makes basic usingtriethylamine followed by addition of compound 23(0.003 mol). The reaction mixture was refluxed until the completion of the reaction. After completion of the reaction, the solvent was evaporated and recrystallized using methanol to obtain the target compounds (45-47).

2-((4-(2-chloro-6-nitrophenoxy) benzylidene)amino)-3-hydroxypropanoic acid (45)

^{1}H NMR (500 MHz, $CDCl_3$) δ 9.30 (s, 1H), 8.05 (m, 1H), 7.65 (m, 1H), 7.58 – 7.45 (m, 2H), 7.02 – 6.88 (m, 2H), 5.87 (s, 1H), 4.21 – 4.19 (m, 2H), 4.21 (m, 1H), 3.30 (s, 3H).^{13}C NMR (125 MHz, $CDCl_3$) δ 173.39, 161.40, 157.35, 144.78, 139.58, 133.44, 132.85, 130.52, 130.30 , 128.41, 127.28, 126.06, 119.96, 119.74, 76.29, 63.06 ; Anal. $C_{16}H_{13}ClN_2O_6$: C, 52.69; H, 3.59; N, 7.68; Found: C, 52.66; H, 3.63; N, 7.71.

2-((4-(2-chloro-6-nitrophenoxy) benzylidene)amino)-3-hydroxybutanoic acid (46)

^{1}H NMR (500 MHz, $CDCl_3$) δ 8.50 (s, 1H), 7.99 (m, 1H), 7.60 – 7.45 (m, 3H), 7.18 – 7.06 (m, 2H), 7.04 (s, 1H), 4.43 (s, 1H), 4.21 – 4.19 (m, 2H), 3.91 (m, 1H), 3.67 (s, 3H), 1.56 (m, 1H),.^{13}C NMR (125 MHz, $CDCl_3$) ä 175.13, 162.59, 157.38, 144.88, 140.31, 133.45, 132.81, 130.49, 130.27, 128.38, 126.85, 126.04, 120.01, 119.61, 81.26, 69.18, 21.08 ; Anal. $C_{17}H_{15}ClN_2O_6$: C, 53.91; H, 3.99; N, 7.40; Found: C, 53.89; H, 4.01; N, 7.44.

2-((4-(2-chloro-6-nitrophenoxy) benzylidene)amino)-3-(4-hydroxyphenyl)propanoic acid (47)

^{1}H NMR (500 MHz, $CDCl_3$) δ 8.78 (s, 1H), 7.89 (m, 1H), 7.61 (m, 1H), 7.53 – 7.38 (m, 2H), 7.24 (m, 1H), 7.10 – 6.92 (m, 2H), 6.84 (m, 1H), 6.80 – 6.66 (m, 2H), 4.39 (m, 1H), 3.78 (s, 3H), 3.57 (s, 1H), 3.28 – 3.01 (m, 2H). ^{13}C NMR (125 MHz, $CDCl_3$) δ 173.57, 163.76, 157.35, 156.71, 144.78, 139.58, 133.44, 132.85, 130.96, 130.75, 130.52, 130.30, 129.42, 128.41, 127.28, 126.06, 119.96, 119.74, 116.07, 115.86, 75.65, 35.94 ; Anal. $C_{22}H_{17}ClN_2O_6$: C, 59.94; H, 3.89; N, 6.35; Found: C, 59.90; H, 3.92; N, 6.39.

Pharmacology

In vitro assays

Estimation of cholinesterase activity : The IC_{50} value of all the compounds was examined on AChE obtained from the electric eel (E.C. 3.1.1.7) and butyrylcholinesterase obtained from human serum (E.C. 3.1.1.8) as per Ellman's method (22). Different concentrations of compounds from 10 nm to 100µm were selected to obtain inhibition of the enzymatic activity. A stock solution of Enzyme 2.5 unit/ ml was prepared. The final assay solution was prepared by mixing 25 µl 2.5 unit/mL of AChE and 10 µl of different concentrations of the compounds, followed by addition of 300µl 0.1 M phosphate buffer (pH 8.0), 50µl of 0.001 M 5,52 - dithiobis(2-nitrobenzoic acid), and 10µl of 0.0075 M of substrate (acetylthiocholine iodide, ATCh or butyrylthiocholine iodide, BTCh, respectively). The reaction was allowed to proceed for 10 min and absorbance measured at 412 nm for every 1 min. The blank assay consisted of all components except AChE to account for the non-enzymatic reaction. The reaction rates were compared, and the percent inhibition due to the increasing concentrations of the compound was calculated. The concentration of each test compound was

recorded in triplicate, and their IC_{50} values were determined graphically from percent inhibition curves. While determining the enzyme kinetics, different substrate concentration was used. The concentration of compound 39 was fixed at its IC_{50}. The Ki value was determined using the Lineweaver and Burk method(24).

DPPH (2, 2-diphenyl -1-picryl -hydrazyl) radical scavenging activity : DPPH assay was used to measure the antioxidant potential of the compound. 100 µl solution of test compound at several concentrations (10 nm to 100 µm) in methanol was mixed with 200 µl of 0.5 mM DPPH solution. After shaking vigorously, it was allowed to stand in the dark for 30 min at room temperature, and the reading was taken at 517 nm.

Propidium iodide displacement assay : Propidium Iodide displacement assay was used to measure the displacement of Propidium Iodide from the PAS of AChE in respect to the test compound. The 5U of the enzyme was prepared in 0.1 mMTris buffer. Different concentration of test compounds was added to the solution and incubated at room temperature for 20 hours. The 20 µM propidium iodide was added, and the fluorescence was measured after 10 min at excitation and emission wavelength 535 and 595 nm respectively (23).

PAMPA- BBB assay : The pore size of acceptor microplates with PVDF membrane was 0.45 mm and was glazed with porcine brain lipid in dodecane and buffer (pH 7.4) was poured in sufficient quantity. Compounds 39 and donepezil were dissolved in DMSO (5 mg/ml) and diluted up to 200 fold. The resulting solution was added to the donor well plate. The acceptor plate was placed cautiously above the donor plate and then incubated (18 h). The amount of drug in donor and acceptor plate was determined in UV (n = 3; scanned for at least five different wavelengths). Validation of PAMPA model was performed using drugs (mentioned in the discussion, purchased commercially) (32).

In vivo and ex vivo studies

Animals : The adult Swiss albino mice weighing 24-28 g were procured from the approved vendors. The protocol of the experiment and the number of mice required were approved by the animal ethical committee (Dean/2017/CAEC/92). Animals were maintained in environmentally controlled temperature (25 ± 2 °C) and humidity (65 ± 5 %RH) with 12 h light/dark cycles, and water ad libitum and commercial rodent feed were freely available.*Experimental design and drug administration*

Test compounds were suspended in 0.3% w/v sodium carboxymethylcellulose (CMC). The behavioural studies were performed in seven groups with each group having six mice as follows: (i) control (ii) vehicle (0.5 ml) (iii) scopolamine hydrobromide (3 mg/kg), (iv) donepezil (plus scopolamine hydrobromide) (1 mg/kg), (v), (vi), and (vii) compound 39 (plus scopolamine hydrobromide) (1, 5, 20 mg/kg respectively). Treatment was given once daily for seven consecutive days to the respective group of animals. Scopolamine hydrobromide was dissolved in distilled water and administer edintraperitoneally to mice after 30 min of drug treatment on the 7th day of the experiment.

Y-maze test: The Y-maze apparatus consists of three arms maze mostly used for the assessment of instant and short working memory in the rodents. After 30 min of 7th day treatment, scopolamine hydrobromide was administered intraperitoneally to all groups of mice except the control group. The mice of each group were kept at the center of the maze and allowed to explore all the three arms. The total arm entries and spontaneous alterations behavior were observed for each mouse over a period of 5 min. The "memory improvement score" can be calculated as % spontaneous alterations rate = (Number of alterations/(total arm entries – 2)) x 100(33).

Passive avoidance test: The experimental protocol was followed as mentioned above and the number of animal and route of drug administration remain the same. The animals were

trained in A rectangular box (48 ×23 × 27 cm;Columbus Instrument,PACS-30) having two compartments with electrifiable grid floor connected to a shock device which delivers scrambled foot shocks. In training phase mice was kept on the platform, and allowed to freely move to explore for 10 s and then allowed to return home, and the latency to descend was calculated. Immediately after this, an unavoidable footshock of 0.5 mA for 10 s was applied, and the mice were returned to the home cage. In the retention test, 24 h after the learning trial the mice were again placed on the platform and the step-down latency was measured. The test was ended when the mice remain on the platform. Acquisition period of 30 s was used for each mice and time of descent during the learning phase and the time during the retention test was measured(34).

Rotarod performance test *:* The same groups of animals used in the Y Maze and passive avoidance test were used for the minimal motor impairment measurement using the rotarod test on the next day. The mice were first trained to stay on a rotating rod at 6 rpm with a diameter of 3.2 cm and the experiment was performed on the same dayto measure the minimal motor impairment. Compound **39** and diazepam (5 mg/kg) were given orally 1h earlier experiment. The latency of mice to fall from the rotating rod was automatically measured using sensors(35).

Neurochemical analysis

Preparation of tissue homogenate : After the completion of the behavioral assessments, mice were sacrificed through the cervical dislocation, and the whole brain was isolated, washed with cold double distilled water, and again rinsed with a pre-cooled normal saline solution. Each whole brain was homogenized with 3 ml of 10 mM phosphate buffered saline (pH 7.4) in Teflon-glass homogenizer on ice-cold bath and centrifuged at 8050 ×g-force for 10 min at 4 ºC.

Lowry method of protein estimation : The alkaline copper solution was prepared as per the prescribed method. 0.2 ml of tissue homogenate and 1 ml of alkaline copper solution was mixed well in a test tube and allowed to stand at room temperature for 10-12 minutes. 0.1 ml of Phenol (Folin and Ciocalteu's) reagent (sd fine-chem limited) was mixed rapidly to the above homogenate mixture within two seconds. The absorbance was taken after 30 minutes at 750 nm and plotted against the standard curve to know per mg protein content of the sample(36).

Ex vivo study for the estimation of AChE : The tissue homogenate was accessed for estimation of AChE using Ellman's method as discussed previously. Firstly the Ellman's reagent was prepared by mixing 15ml of 0.1 M phosphate buffer (pH 7.4), 500 µl of DTNB, and 100 µl substrate. 300 µl of this solution was pipet out in the cuvette of 96 well microplates. Then 10 µl of supernatant was added to it, and the absorbance was measured at 412 nm, and the rate of hydrolysis was measured as Hydrolysed ACh/min/mg of protein(29).

Lipid peroxidation assay (Thiobarbituric acid reactive substances method) : The tissue homogenate was mixed with an equal amount of 0.1 M phosphate buffer pH 7.4 and incubated at 37 °C for 2 h. To the incubated mixture 10% cold trichloroacetic acid was added. The mixture was centrifuged at 1000 rpm for 1 min. The supernatant (1 ml) was taken in a test tube and mix with equal amount of 0.67% of TBA. The test tube was boiled for in water bath for 10 minutes, and an equal amount (1 ml) of double distilled water was added, and optical density of the solution was taken at 532 nm, and the absorbance was converted into the no. of moles of MDA/mg protein (37).

Estimation of catalase activity : 250 µl of the mixture was taken from a mixture of 1.95 ml of phosphate buffer (pH 7) and 1 ml of 30mM hydrogen peroxide solution added to the cuvette of the microplate. 5 µl of supernatant was added to it, and the result was expressed as hydrogen peroxide decomposed/min/mg protein(38).

Reduced Glutathione assay *:* 0.01 M DTNB was added to the mixture of homogenate and 4% sulphosalicylic acid which were earlier centrifuged

for 1200 rpm for 15 minutes at 4 °C in phosphate buffer and estimated at 412 nm. The standard GSH curve was plotted, and concentration was measured in µmol of GSH /mg of protein (39).

Estimation of nitrite : Nitrite was estimated using the Griess reagent (an equal mixture of 0.1% aqueous solution of napthylethylenediamine and solution of 1% sulphanilamide in 5% phosphoric acid). 250 µl of Griess reagent and 50 µl of supernatant were added in the well of the microplate. The standard curve of nitrite concentration was calculated using a sodium nitrite was plotted, and the nitrite level concentration in the sample was expressed as mg/ml(38).

Superoxide dismutase assay : Aqueous solution of 0.5 ml hydroxylamine hydrochloride (pH 6.0) was added to the solution containing 50 mM sodium carbonate (pH 10.2) and 0.1 mM EDTA, and 96 mM of Nitro-blue tetrazolium (NBT). 0.05 mL of homogenate was added to this mixture, and the change in absorbance was recorded at 560 nm per 30 s interval for 2 min. Results were expressed as SOD unit/mg protein.

Conflict of interest

The authors declare no conflict of interest.

Acknowledgments

The authors gratefully acknowledge the Indian Institute of Technology (Banaras Hindu University), Varanasi for the financial support and providing necessary infrastructural facilities to carry out the experiments. We are also thankful to the Department of Health Research, Ministry of Health and Family Welfares for approving Young Scientist Grant in newer areas of Drugs Chemistry (V25011/215-HRD/2016-HR).

References

1. Wolters, F. J. and Ikram, M. A. (2018) Epidemiology of Dementia: The Burden on Society, the Challenges for Research *Biomarkers for Alzheimer's Disease Drug Development*, pp. 3-14 (Springer).
2. Organization, W. H. (2018) Towards a dementia plan: a WHO guide.
3. Petersen, R. C. (2018) How early can we diagnose Alzheimer disease (and is it sufficient)?: The 2017 Wartenberg lecture, *Neurology*, 91, 395-402.
4. Hasselmo, M. E. (2006) The role of acetylcholine in learning and memory, *Current opinion in neurobiology*, 16, 710-715.
5. Shrivastava, S. K., Sinha, S. K., Srivastava, P. et al. (2018) Design and development of novel p-aminobenzoic acid derivatives as potential cholinesterase inhibitors for the treatment of Alzheimer's disease, *Bioorganic chemistry*.
6. Coloviæ, M. B., Krstiæ, D. Z., Lazareviæ-Pašti, T. D., Bond•iæ, A. M. and Vasiæ, V. M. (2013) Acetylcholinesterase inhibitors: pharmacology and toxicology, *Current neuropharmacology*, 11, 315-335.
7. Darvesh, S., Hopkins, D. A. & Geula, C. (2003) Neurobiology of but yrylcholines terase, *Nature Reviews Neuroscience*, 4, 131.
8. Luca, M., Luca, A. and Calandra, C. (2015) The Role of Oxidative Damage in the Pathogenesis and Progression of Alzheimer's Disease and Vascular Dementia, *Oxidative medicine and cellular longevity*, 2015, 504678-504678.
9. Mecocci, P., Boccardi, V., Cecchetti, R. et al. (2018) A Long Journey into Aging, Brain Aging, and Alzheimer's Disease Following the Oxidative Stress Tracks, *Journal of Alzheimer's Disease*, 62, 1319-1335.
10. Oset-Gasque, M. J. S. and Marco-Contelles, J. (2018) Alzheimer's Disease, the "One-Molecule, One-Target" Paradigm, and the Multitarget Directed Ligand Approach (ACS Publications).
11. Özbey, F., Taslimi, P., Gülçin, Ý. et al. (2016) Synthesis of diaryl ethers with acetylcholinesterase, butyrylcholinesterase

and carbonic anhydrase inhibitory actions, *Journal of enzyme inhibition and medicinal chemistry*, 31, 79-85.

12. Andersson, C. D., Forsgren, N., Akfur, C. et al. (2013) Divergent structure–activity relationships of structurally similar acetylcholinesterase inhibitors, *Journal of medicinal chemistry*, 56, 7615-7624.

13. Dolles, D., Hoffmann, M., Gunesch, S. et al. (2018) Structure–Activity Relationships and Computational Investigations into the Development of Potent and Balanced Dual-Acting Butyrylcholinesterase Inhibitors and Human Cannabinoid Receptor 2 Ligands with Pro-Cognitive in Vivo Profiles, *Journal of medicinal chemistry*, 61, 1646-1663.

14. Koelle, G. (1963) Handbuch der experimentellen Pharmakologie, Ergänzungswerk, XV, *Cholinesterases and anticholinesterase agents. Berlin-Göttingen-Heidelberg: Springer 1963a. Google Scholar*.

15. Vanucci-Bacqué, C., Camare, C., Carayon, C. et al. (2016) Synthesis and evaluation of antioxidant phenolic diaryl hydrazones as potent antiangiogenic agents in atherosclerosis, *Bioorganic & medicinal chemistry*, 24, 3571-3578.

16. Andersson, C. D., Hillgren, J. M., Lindgren, C. et al. (2015) Benefits of statistical molecular design, covariance analysis, and reference models in QSAR: a case study on acetylcholinesterase, *Journal of computer-aided molecular design*, 29, 199-215.

17. Selvaraj, C., Tripathi, S. K., Reddy, K. K. and Singh, S. K. (2011) Tool development for Prediction of pIC 50 values from the IC 50 values-A pIC 50 value calculator, *Current Trends in Biotechnology & Pharmacy*, 5.

18. Langdon, S. R., Ertl, P. and Brown, N. (2010) Bioisosteric replacement and scaffold hopping in lead generation and optimization, *Molecular Informatics*, 29, 366-385.

19. Cho, A. E., Guallar, V., Berne, B. J. and Friesner, R. (2005) Importance of accurate charges in molecular docking: quantum mechanical/molecular mechanical (QM/MM) approach, *Journal of computational chemistry*, 26, 915-931.

20. Bowers, K. J., Chow, D. E., Xu, H. et al. (2006) Scalable algorithms for molecular dynamics simulations on commodity clusters, Paper presented at the *SC 2006 conference, proceedings of the ACM/IEEE*.

21. Williamson, A. (1850) XLV. Theory of ætherification, *The London, Edinburgh, and Dublin philosophical magazine and journal of science*, 37, 350-356.

22. Ellman, G. L., Courtney, K. D., Andres Jr, V. and Featherstone, R. M. (1961) A new and rapid colorimetric determination of acetylcholinesterase activity, *Biochemical pharmacology*, 7, 88-95.

23. Peauger, L., Azzouz, R., Gembus, V. et al. (2017) Donepezil-based central acetylcholinesterase inhibitors by means of a “bio-oxidizable” prodrug strategy: design, synthesis, and in vitro biological evaluation, *Journal of medicinal chemistry*, 60, 5909-5926.

24. Lineweaver, H. & Burk, D. (1934) The determination of enzyme dissociation constants, *Journal of the American chemical society*, 56, 658-666.

25. Brand-Williams, W., Cuvelier, M.-E. and Berset, C. (1995) Use of a free radical method to evaluate antioxidant activity, *LWT-Food science and Technology*, 28, 25-30.

26. Ottaviani, G., Martel, S. & Carrupt, P.-A. (2006) Parallel artificial membrane permeability assay: a new membrane for the fast prediction of passive human skin permeability, *Journal of medicinal chemistry*, 49, 3948-3954.

27. Shrivastava, S. K., Sinha, S. K., Srivastava, P. et al. (2019) Design and development of novel p-aminobenzoic acid derivatives as potential cholinesterase inhibitors for the treatment of Alzheimer's disease, *Bioorganic chemistry*, 82, 211-223.

28. Srivastava, P., Tripathi, P. N., Sharma, P. et al. (2019) Design and development of some phenyl benzoxazole derivatives as a potent acetylcholinesterase inhibitor with antioxidant property to enhance learning and memory, *European journal of medicinal chemistry*, 163, 116-135.

29. Shrivastava, S. K., Srivastava, P., Upendra, T., Tripathi, P. N. and Sinha, S. K. (2017) Design, synthesis and evaluation of some N-methylenebenzenamine derivatives as selective acetylcholinesterase (AChE) inhibitor and antioxidant to enhance learning and memory, *Bioorganic & medicinal chemistry*, 25, 1471-1480.

30. Suvire, F. D., Sortino, M., Kouznetsov, V. V. et al. (2006) Structure–activity relationship study of homoallylamines and related derivatives acting as antifungal agents, *Bioorganic & medicinal chemistry*, 14, 1851-1862.

31. Feng, B., Lu, L. Q., Chen, J. R. et al. (2018) Umpolung of Imines Enables Catalytic Asymmetric Regio reversed [3+ 2] Cycloadditions of Iminoesters with Nitroolefins, *Angewandte Chemie International Edition*, 57, 5888-5892.

32. Di, L., Kerns, E. H., Fan, K., Mcconnell, O. J. & Carter, G. T. (2003) High throughput artificial membrane permeability assay for blood–brain barrier, *European journal of medicinal chemistry*, 38, 223-232.

33. Kwon, S.-H., Lee, H.-K., Kim, J.-A. et al. (2010) Neuroprotective effects of chlorogenic acid on scopolamine-induced amnesia via anti-acetylcholinesterase and anti-oxidative activities in mice, *European journal of pharmacology*, 649, 210-217.

34. Rush, D. K. (1988) Scopolamine amnesia of passive avoidance: a deficit of information acquisition, *Behavioral and Neural Biology*, 50, 255-274.

35. Seth, A., Sharma, P. A., Tripathi, A. et al. (2018) Design, synthesis, evaluation and molecular modeling studies of some novel N-substituted piperidine-3-carboxylic acid derivatives as potential anticonvulsants, *Medicinal Chemistry Research*, 27, 1206-1225.

36. Lowry, O. H., Rosebrough, N. J., Farr, A. L. & Randall, R. J. (1951) Protein measurement with the Folin phenol reagent, *Journal of biological chemistry*, 193, 265-275.

37. Wills, E. (1966) Mechanisms of lipid peroxide formation in animal tissues, *Biochemical Journal*, 99, 667.

38. Kulshreshtha, A. & Piplani, P. (2016) Ameliorative effects of amide derivatives of 1, 3, 4-thiadiazoles on scopolamine induced cognitive dysfunction, *European journal of medicinal chemistry*, 122, 557-573.

39. Jollow, D., Mitchell, J., Zampaglione, N. A. and Gillette, J. (1974) Bromobenzene-induced liver necrosis. Protective role of glutathione and evidence for 3, 4-bromobenzene oxide as the hepatotoxic metabolite, *Pharmacology*, 11, 151-169.

40. Beniddir, M., Simonin, A.-L., Martin, M.-T. et al. (2009) *Turrianes from Kermadecia rotundifolia as new acetylcholinesterase inhibitors*.

41. Wu, B., Ohlendorf, B., Oesker, V. et al. (2015) Acetylcholinesterase inhibitors from a marine fungus Talaromyces sp. strain LF458, *Marine biotechnology*, 17, 110-119.